# AUTHOR QUERY FORM

| | | |
|---|---|---|
| ELSEVIER | **Journal: EPSL**<br><br>**Article Number: 10257** | **Please e-mail or fax your responses and any corrections to:**<br>**E-mail: corrections.esnl@elsevier.spitech.com**<br>**Fax: +1 61 9699 6721** |

Dear Author,

Any queries or remarks that have arisen during the processing of your manuscript are listed below and highlighted by flags in the proof. Please check your proof carefully and mark all corrections at the appropriate place in the proof (e.g., by using on-screen annotation in the PDF file) or compile them in a separate list.

For correction or revision of any artwork, please consult http://www.elsevier.com/artworkinstructions.

**Articles in Special Issues:** Please ensure that the words 'this issue' are added (in the list and text) to any references to other articles in this Special Issue.

**Uncited references:** References that occur in the reference list but not in the text – please position each reference in the text or delete it from the list.

**Missing references:** References listed below were noted in the text but are missing from the reference list – please make the list complete or remove the references from the text.

| Location in article | Query / remark<br>Please insert your reply or correction at the corresponding line in the proof |
|---|---|
| Q1 | Keywords were taken from the manuscript draft. Please check if appropriate. |
| Q2 | Please check doi. |
| Q3 | Please check doi. |
| Q4 | Please check doi. |
| Q5 | Please check doi. |
| Q6 | Please check doi. |
| Q7 | Please check doi. |
| Q8 | Please check doi. |
| Q9 | Please check doi. |
| Q10 | Please check doi. |
| Q11 | Please check doi. |
| Q12 | Please check doi. |
| Q13 | Please check doi. |

**Electronic file usage**

Sometimes we are unable to process the electronic file of your article and/or artwork. If this is the case, we have proceeded by:

☐ Scanning (parts of) your article ☐ Rekeying (parts of) your article ☐ Scanning the artwork

Thank you for your assistance.

Earth and Planetary Science Letters xxx (2010) xxx–xxx

Contents lists available at ScienceDirect

Earth and Planetary Science Letters

journal homepage: www.elsevier.com/locate/epsl

# North Atlantic millennial-scale climate variability 910 to 790 ka and the role of the equatorial insolation forcing

Patrizia Ferretti [a,b,*], Simon J. Crowhurst [a], Michael A. Hall [a], Isabel Cacho [b]

[a] The Godwin Laboratory for Palaeoclimate Research, Department of Earth Sciences, University of Cambridge, Downing Street, Cambridge CB2 3EQ, United Kingdom
[b] GRC Marine Geosciences, Department of Stratigraphy, Palaeontology and Marine Geosciences, Faculty of Geology, University of Barcelona, C/Martí i Franqués, s/n, E-08028 Barcelona, Spain

UNCORRECTED PROOF

ARTICLE INFO

*Article history:*
Received 27 July 2009
Received in revised form 5 February 2010
Accepted 10 February 2010
Available online xxxx

Editor: M.L. Delaney

*Keywords:*
North Atlantic
Early Pleistocene
foraminifera
stable isotopes
millennial
insolation
IODP
Site U1313

ABSTRACT

The Mid-Pleistocene transition (MPT) was the time when quasi-periodic (~100 kyr), high-amplitude glacial variability developed in the absence of any significant change in the character of orbital forcing, leading to the establishment of the characteristic pattern of late Pleistocene climate variability. It has long been known that the interval around 900 ka BP stands out as a critical point of the MPT, when major glaciations started occurring most notably in the northern hemisphere. Here we examine the record of climatic conditions during this significant interval, using high-resolution stable isotope records from benthic and planktonic foraminifera from a sediment core in the North Atlantic (Integrated Ocean Drilling Program Expedition 306, Site U1313). We have considered the time interval from late in Marine Isotope Stage (MIS) 23 to MIS 20 (910 to 790 ka). Our data indicate that interglacial MIS 21 was a climatically unstable period and was broken into four interstadial periods, which have been identified and correlated across the North Atlantic region. These extra peaks tend to contradict previous studies that interpreted the MIS 21 variability as consisting essentially of a linear response to cyclical changes in orbital parameters. Cooling events in the surface record during MIS 21 were associated with low benthic carbon isotope excursions, suggesting a coupling between surface temperature changes and the strength of the Atlantic meridional overturning circulation. Time series analysis performed on the whole interval indicates that benthic and planktonic oxygen isotopes have significant concentrations of spectral power centered on periods of 10.7 kyr and 6 kyr, which is in agreement with the second and forth harmonic of precession. The excellent correspondence between the foraminifera $\delta^{18}O$ records and insolation variations at the Equator in March and September suggests that a mechanism related to low-latitude precession variations, advected to the high latitudes by tropical convective processes, might have generated such a response. This scenario accounts for the presence of oscillations at frequencies equal to precession harmonics at Site U1313, as well as the occurrence of higher amplitude oscillations between the MIS22/21 transition and most of MIS 21, times of enhanced insolation variability.

© 2010 Elsevier B.V. All rights reserved.

## 1. Introduction

The Mid-Pleistocene transition (MPT) represents perhaps the most important climate transition in the Quaternary period, yet it is one of the most poorly understood. Although the exact timing and mechanism of the onset of the “100 kyr” regime remain a matter of debate, it is well established that the overall periodicity of the glacial–interglacial cycles changed from a dominant 41 kyr obliquity periodicity prior to ~0.9 Ma to a dominant late Pleistocene 100 kyr variance. This change in the frequency domain was associated with an increase in the amplitude of global ice volume variations that, superimposed on a long-term climatic trend towards more glacial conditions over millions of years, produced some of the most extreme glaciations recorded (Shackleton and Opdyke, 1976; Pisias and Moore, 1981; Ruddiman et al., 1989; ; Imbrie et al., 1993).

The intensification and prolongation of the glacial–interglacial cycles appear not to have occurred synchronously: a significant increase in global ice volume was centered at ~920 ka and lasted ~40 kyr, followed by a prolonged “interim” period (~280 kyr) before the abrupt increase in the amplitude of the 100 kyr cycles at ~642 ka (Mudelsee and Schulz, 1997). Within this complex interval of climatic evolution, the cold Marine Isotope Stage (MIS) 22 (~870–900 ka) is perhaps the single most profound episode of environmental change. Collective evidence from the northern continents indicates that MIS 22 is the first prominent cooling event and glacioeustatic lowstand of the Pleistocene. Alpine valley glaciers reached their first Pleistocene maximum southward expansion during MIS 22 (Muttoni et al., 2003; Muttoni et al., 2007). A large increase in North American ice volume occurred between the late

* Corresponding author. GRC Marine Geosciences, Department of Stratigraphy, Palaeontology and Marine Geosciences, Faculty of Geology, University of Barcelona, C/Martí i Franqués, s/n, E-08028 Barcelona, Spain. Tel.: +34 93 4020177; fax: +34 93 4021340.
*E-mail addresses:* pf233@cam.ac.uk, pferretti@ub.edu (P. Ferretti).

0012-821X/$ – see front matter © 2010 Elsevier B.V. All rights reserved.
doi:10.1016/j.epsl.2010.02.016

Matuyama and the Brunhes chrons, at around MIS 22 (Barendregt and Irving, 1998). The glacioeustatic effects of ice-build up during this glaciation caused a substantial sea-level fall. Shallow marine sediments off Japan indicate that eustatic sea-level dropped during MIS 22 and was 20–30 m lower than during stage 28 (Kitamura and Kawagoe, 2006). Thicker and sandier loess deposits in northern Eurasia signal the onset of severe palaeoclimatic conditions in such a distinct way that the base of MIS 21 has been identified as a convenient and effective marker for recognising the Early–Middle Pleistocene boundary in loess-palaeosol sequences (Heslop et al., 2002; Dodonov, 2005). In the Chinese Loess Plateau, monsoon wind strength, estimated from the grain size of the wind-blown lithogenic sediments, increased during MIS 22 (Sun et al., 2006).

Significant changes in the oceanic circulation occurred at the same time. Sea surface temperature records from the North Atlantic, eastern tropical Atlantic and eastern equatorial Pacific show that the major cooling event of the MPT was associated with MIS 24–22 (Ruddiman et al., 1989; Schefuβ et al., 2004; McClymont and Rosell-Mele´, 2005). Deep-water carbon isotopic signals from the North Atlantic and sub-Antarctic regions became very depleted in $^{13}C$ during MIS 22 (Raymo et al., 1990; Hodell et al., 2003; Ferretti et al., 2005), reflecting profound changes in deep-water circulation and probably a more global event connected to a transfer of carbon from the organic to inorganic pools in the ocean (Clark et al., 2006). In the deep western North Atlantic, almost pure Antarctic Bottom Water was detected for the first time within the mid-Pleistocene shift during MIS 24–22, implying pronounced changes in the balance between northern and southern source waters (Ferretti et al., 2005). A similar stagnation of bottom-water circulation was also detected in the South Atlantic at the same time (Schmieder et al., 2000).

In this paper, we focus on this initial main event of the mid-Pleistocene climate shift as defined by Mudelsee and Schulz (1997)–the build up of the first distinctly larger Northern Hemisphere ice sheets–and investigate the climatic evolution of a sector of the North Atlantic Ocean from late MIS 23 to MIS 20. This interval of time has often been considered to be important in relation to long-term Milankovitch-scale climate variability. In contrast, here, special emphasis will be placed on assessing the presence and the characteristics of the suborbital-scale variability in North Atlantic sea surface and deep-water hydrography. Appealing evidence suggests that millennial-scale climate variability is amplified during times of intense forcing changes (Alley et al., 1999), but this rapid variability has not been thoroughly explored yet at the time when the major changes in climate periodicity occurred.

Previous studies of polar ice cores, marine and terrestrial records have shown that millennial and submillennial climate perturbations (e.g. Dansgaard-Oeschger Cycles) have punctuated the long-term climate development on glacial–interglacial time scales during the last 100 kyr and were connected with changes in the operational modes of the Atlantic meridional overturning circulation (AMOC), a critical component of the global climate system (e.g. Alley (2007) and references therein). Here we investigate the behavior of the climate system in the millennial band under a different climatic framework in order to explore the processes operating when the climate sensitivity to orbital forcing was different from that of the late Pleistocene. We will show that, although the period analysed in this study was a time of transition and development, some of the features and mechanisms attributed to millennial-scale variability were already recognisable and operating at this time. We will also suggest that some of the millennial-scale variability observed at our North Atlantic site was influenced by the equatorial and tropical regions, confirming the important role played by these regions in the response of the climate system to the astronomical forcing.

## 2. Regional setting, materials and method

Site U1313 was raised from a water depth of 3426 m at 41°00′N 32°58′W, on the upper middle western flank of the Mid-Atlantic Ridge during Integrated Ocean Drilling Program Expedition (IODP) 306 (Expedition 306 Scientists, 2006) (Fig. 1). Although today this site is located south of the North Atlantic Current (NAC), recent studies using surface drifters indicate that the surface waters in this region are derived from the NAC (Fratantoni, 2001; Reverdin et al., 2003). Moreover, it is in the path of the deep North Atlantic Deep Water (NADW) western boundary current as it exits the northernmost Atlantic.

UNCORRECTED PROOF

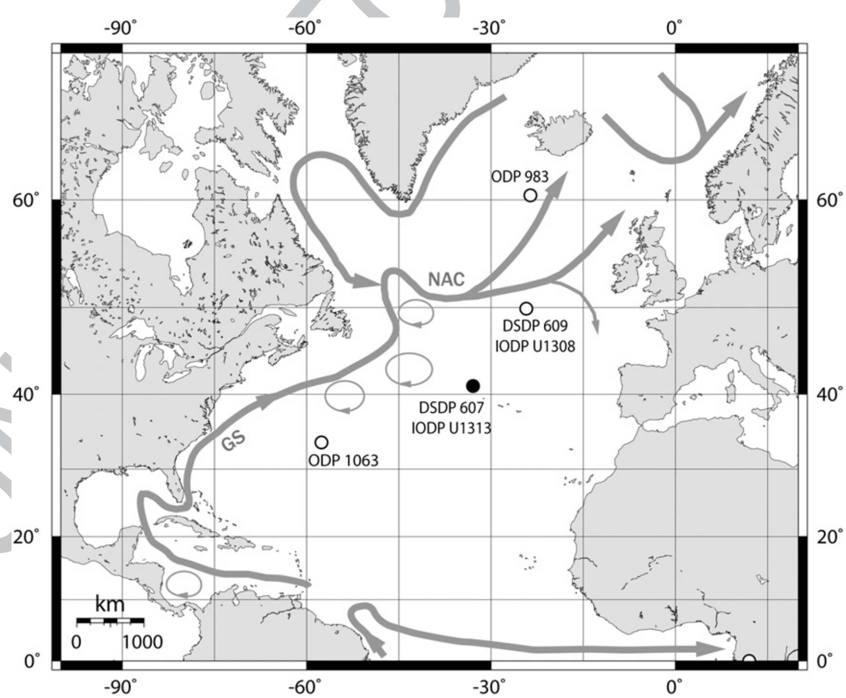


**Fig. 1.** Map showing the locations of the cores investigated and discussed in this study: ODP Site 983 (60°23′N 23°38′W, 1985 m water depth), ODP Site 1063 (33°41′N 57°36′W, 4584 m water depth), IODP Site U1308 (49°53′N 24°14′W, 3872 m water depth) and IODP Site U1313 (41°00′N 32°58′W, 3426 m water depth). Major surface water currents are from Fratantoni (2001): GS = Gulf Stream; NAC = North Atlantic Current.

Please cite this article as: Ferretti, P., et al., North Atlantic millennial-scale climate variability 910 to 790 ka and the role of the equatorial insolation forcing, Earth Planet. Sci. Lett. (2010), doi:10.1016/j.epsl.2010.02.016

Site U1313 constitutes a reoccupation of Deep Sea Drilling Project (DSDP) Site 607, which has provided many important advances in palaeoceanography during the last 20 years (Raymo et al., 1989; Ruddiman et al., 1989; Ruddiman et al., 1986; Raymo et al., 2004; ), including yielding valuable insights into the long-term surface and deep-water circulation patterns in the mid-latitude North Atlantic. In order to examine in detail the suborbital variation in the sea surface and deep hydrography at the same location during a critical interval of climate evolution, analyses of Site U1313 samples were performed at higher resolution (1- or 2-cm intervals) than those originally carried out at Site 607. In addition, modern drilling techniques and multiple coring applied during IODP Expedition 306 improved the continuity of the stratigraphic section obtained at Site U1313 in relation to the older DSDP Site 607, which was recovered before the development of shipboard composite sections.

The working half was cut into 1-cm slices between 38.40 and 43.32 m composite depth (or 38.41 and 43.44 revised meters composite depth; correction by Gary Acton, personal communication). Samples were covered with reverse osmosis water (RO), disaggregated in an orbital shaker, then washed through a 63 µm sieve using RO water, and finally the residuals were dried overnight in an oven at 50 °C. The deep-water record was obtained from *Cibicidoides wuellerstorfi*, picked from the fraction >150µm, an epifaunal benthic foraminiferal species (from now onwards simply "benthic") which has been shown to be the most reliable indicator of the $\delta^{13}C$ of dissolved $CO_2$ in the bottom water (Belanger et al., 1981). At Site U1313, *C. wuellerstorfi* was continuously present and well preserved throughout the interval analysed in this study, and we were able to produce a benthic $\delta^{13}C$ record at the same resolution as the planktonic stable isotope signal. About five specimens were used for each analysis. For the surface water record, we chose to analyse *Globigerina bulloides*, because this species has a depth preference within the upper 100 m (Be', 1977) and is therefore well qualified to be a recorder of surface water conditions. In addition, this planktonic foraminiferal species (from now onwards simply "planktonic") is present throughout the record. To minimize the effects of ontogenetic development on the isotopic composition of the tests, specimens were selected from a controlled size-range, 300–355 µm. Thirty specimens were used for each analysis in order to constrain the intraspecific variability; the use of this relatively large number also reduces analytical noise.

Samples were crushed and cleaned in 3% hydrogen peroxide solution before the isotopic analyses, which were carried out at the Godwin Laboratory (University of Cambridge). Measurements of the isotopic composition of carbon dioxide released from the foraminiferal carbonate using a MULTIPREP system were performed on a VG PRISM (for benthic foraminifera) and a VG SIRA (for planktonic foraminifera) mass spectrometers. Calibration to the Vienna Peedee Belemnite standard was through the NBS19 standard (Coplen, 1995), and the analytical precision was better than 0.08‰ for $\delta^{18}O$ and 0.06‰ for $\delta^{13}C$.

The age model for Site U1313 was constructed by correlating the benthic $\delta^{18}O$ to the stacked $\delta^{18}O$ record of Lisiecki and Raymo (2005). The age control points used are listed in Table 1. According to our age model, the record spans the time interval from 788 ka to 912 ka, and the sample spacing provides a resolution ranging from less than 350 years during MIS 20 and 22 to about 250 years during MIS 21.

Time series analyses were used to estimate the variance distribution as a function of frequency, as well as the coherence and phase relationships between records. Cross-spectral analysis of the proxy data sets was undertaken using the ARAND software package (Howell et al., 2006) and applying Blackman–Tukey methods (Jenkins and Watts, 1968). Confirmatory analyses and bandpass filtering were carried out using Analyseries (Paillard et al., 1996), and Redfit (Schulz and Mudelsee, 2002) was used to help examine the statistical significance of particular peaks. Correlation coefficients for cross-correlations were calculated using IBM SPSS software.

**Table 1**
Age control points for correlating IODP Site U1313 to the Lisiecki and Raymo (2005) stack. Between control points, age is estimated by linear interpolation.

| Age (ka) | Depth (rmcd) |
|---|---|
| 788 | 38.42 |
| 810 | 39.72 |
| 832 | 40.37 |
| 852 | 41.30 |
| 866 | 41.70 |
| 912 | 43.41 |

## 3. Results

The oxygen isotope record for *G. bulloides* and *C. wuellerstorfi*, together with the benthic carbon isotope data, document suborbital-scale climate variations at different time scales over the interval between late in MIS 23 and MIS 20 (Fig. 2). The longer periodicity components of our proxy records have been emphasized in Fig. 2 by a Gaussian interpolation of the isotope data using a 15 kyr window width (effectively a 10 kyr threshold low-pass filter), showing that the higher amplitude oscillations are prevalent during MIS 21. In detail, the isotope records show that MIS 21 stands out as an interglacial interrupted by abrupt cool periods. According to the benthic $\delta^{18}O$, which provides a standard stratigraphy for the core, and within the limitations of our age model, at least four events of light oxygen isotope values and benthic $\delta^{13}C$ enrichment are documented in this interval and centred at ca. 860, 848, 838 and 824 ka. We observe a trough-to-peak range of 0.7–1‰ in the planktonic $\delta^{18}O$ record during these events. If these suborbital oscillations are entirely driven by sea surface temperature (SST) changes, they correspond to oscillations of about 3° to 4 °C (Shackleton, 1974). Although SST variability is the simplest explanation for the planktonic $\delta^{18}O$ oscillations, it must be kept in mind that, while the $\delta^{18}O$ of *G. bulloides* records the full glacial–interglacial range of SST change in the North Atlantic, it is also affected by variations in the $\delta^{18}O$ of surface waters. In addition, shifts in the season of maximum flux during glacial and interglacial periods might have also played a role in the $\delta^{18}O$ variability of *G. bulloides*.

In order to emphasize the millennial-scale variability in the isotope signal from Site U1313, we have subtracted the Gaussian interpolation of the isotope data from the full record; in doing this, we aim to isolate the higher frequency component of the signal, and to examine whether changes occurred in the amplitude and duration of suborbital variations during the time interval analysed. The results are shown in Fig. 3. A comparison of the shared high-amplitude variance (confirmed by the spectral analyses, as described below) between residuals from the benthic and planktonic isotope records suggests a high signal-to-noise ratio, adding confidence to the interpretation that the residual variability contains the high-resolution component of the measured records. The amplitude of the suborbital variations in the planktonic $\delta^{18}O$ (0.5–0.8‰) is slightly smaller than the variability identified at the Bermuda Rise during MIS 3 (Keigwin and Boyle, 1999), and similar to the amplitude of variations observed during MIS 5 at Site 1059 (Oppo et al., 2001) and MIS 11 at Site 1056 (Chaisson et al., 2002) in the western subtropical North Atlantic.

Cross-spectral analyses of the benthic and planktonic $\delta^{18}O$ residuals indicate significant concentrations of spectral power around a 10.7 kyr periodicity (Fig. 4a). Variance is also centred on the 6-kyr period, but with power far stronger in the benthic $\delta^{18}O$ than in planktonic $\delta^{18}O$, although a weak peak at this periodicity is identifiable in the planktonic $\delta^{18}O$ as well. The 6-kyr peak in the planktonic record might be considered of marginal or no significance on its own. However, in the context of a climatological setting where the exact frequency is reasonably confidently known to affect the environment, the strong presence of this periodicity in the benthic $\delta^{18}O$ carries more weight on the significance of the planktonic

ARTICLE IN PRESS



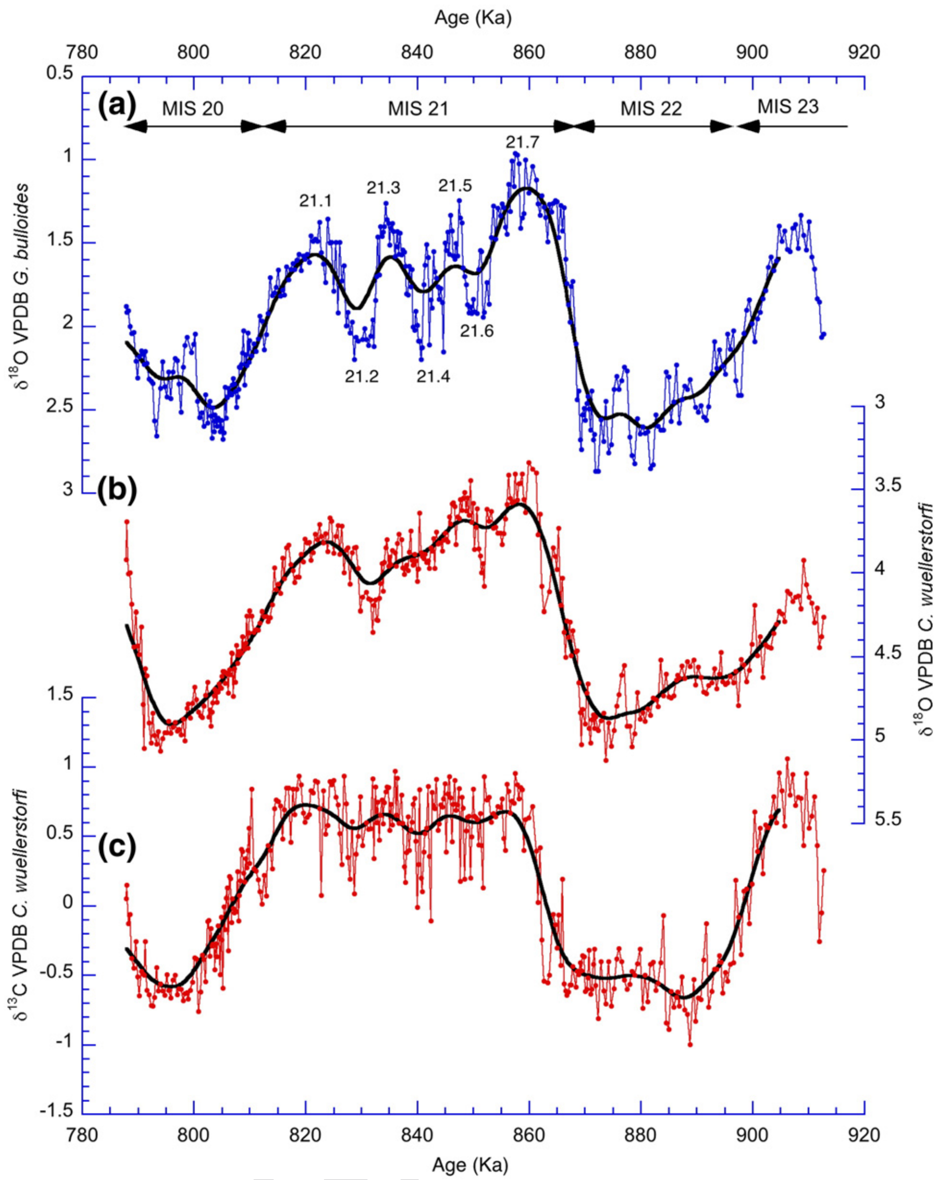


**Fig. 2.** Stable isotope records from IODP Site U1313. (a) *Globigerina bulloides* $\delta^{18}$O; (b) *Cibicidoides wuellerstorfi* $\delta^{18}$O; (c) *C. wuellerstorfi* $\delta^{13}$C (thin lines with data point markers). The $\delta^{18}$O values of *C. wuellerstorfi* were adjusted by +0.64‰ to bring them into presumed oxygen isotopic equilibrium with ambient sea water (Shackleton and Opdyke, 1973). Also shown is the Gaussian interpolation of the three isotopic records using a 15 kyr Gaussian window (thick line without marker). A revised definition of MIS 21 substages is reported.

peak. Benthic and planktonic $\delta^{18}$O residuals are coherent above the 95% confidence level at both periodicities. The phase relationship at 10.7 kyr suggests a phase offset between the two parameters of about 38.8°, which at this periodicity is equivalent to ca. 1.1 kyr, with benthic leading planktonic $\delta^{18}$O residuals. Although the 6 kyr periodicity should be interpreted cautiously, the estimated phase offset is 23.5°, which would correspond to a ca. 400 year lead of benthic $\delta^{18}$O to planktonic $\delta^{18}$O.

Fig. 4a indicates that some variance in the $\delta^{18}$O was also present at higher frequencies, but was dwarfed by the 10.7 and 6 kyr periodicities. The benthic $\delta^{18}$O residual record displays peaks centered at 3.8, 2.9, 2.4, and 2 kyr, whereas the planktonic $\delta^{18}$O variance is concentrated at around 4, 3 and 2 kyr. Although there appears to be spectral power in both parameters at periodicities of ~4, ~3 and 2 kyr, coherency is not high at these frequency bands and the phase estimate would therefore be unreliable. This higher frequency component of climatic variability identified at Site U1313, falling within the 2–4 kyr range, encompasses periodicities that have also been reported in North Atlantic records from the late Pleistocene (Chapman and Shackleton, 1998, 1999; Oppo et al., 1998).

Cross-spectral analysis of the benthic $\delta^{13}$C and planktonic $\delta^{18}$O residuals confirms significant variance of around 10.7 kyr periodicity in the planktonic $\delta^{18}$O and 11.5 kyr in the benthic $\delta^{13}$C, which, given the bandwidth, are likely to represent the same cyclicity (Fig. 4b). Substantial variance is also present at the 3.7 and 1.9 kyr periods in the benthic $\delta^{13}$C residuals. At the 10.7–11.5 kyr periodicity the coherence is just below the 80% confidence criterion, indicating that the phase estimate is statistically unreliable due to a lack of coherence between the parameters. Given the poor coherence and the difference in the absolute spectral peaks, these data are not sufficient to establish a phase relationship between these variables at this periodicity in the interval analysed.

## 4. Discussion

### 4.1. Climate instability during MIS 21

At the relatively longer suborbital periodicities, rapid increases in the oxygen isotope records at Site U1313 break the interglacial MIS 21 into

Please cite this article as: Ferretti, P., et al., North Atlantic millennial-scale climate variability 910 to 790 ka and the role of the equatorial insolation forcing, Earth Planet. Sci. Lett. (2010), doi:10.1016/j.epsl.2010.02.016

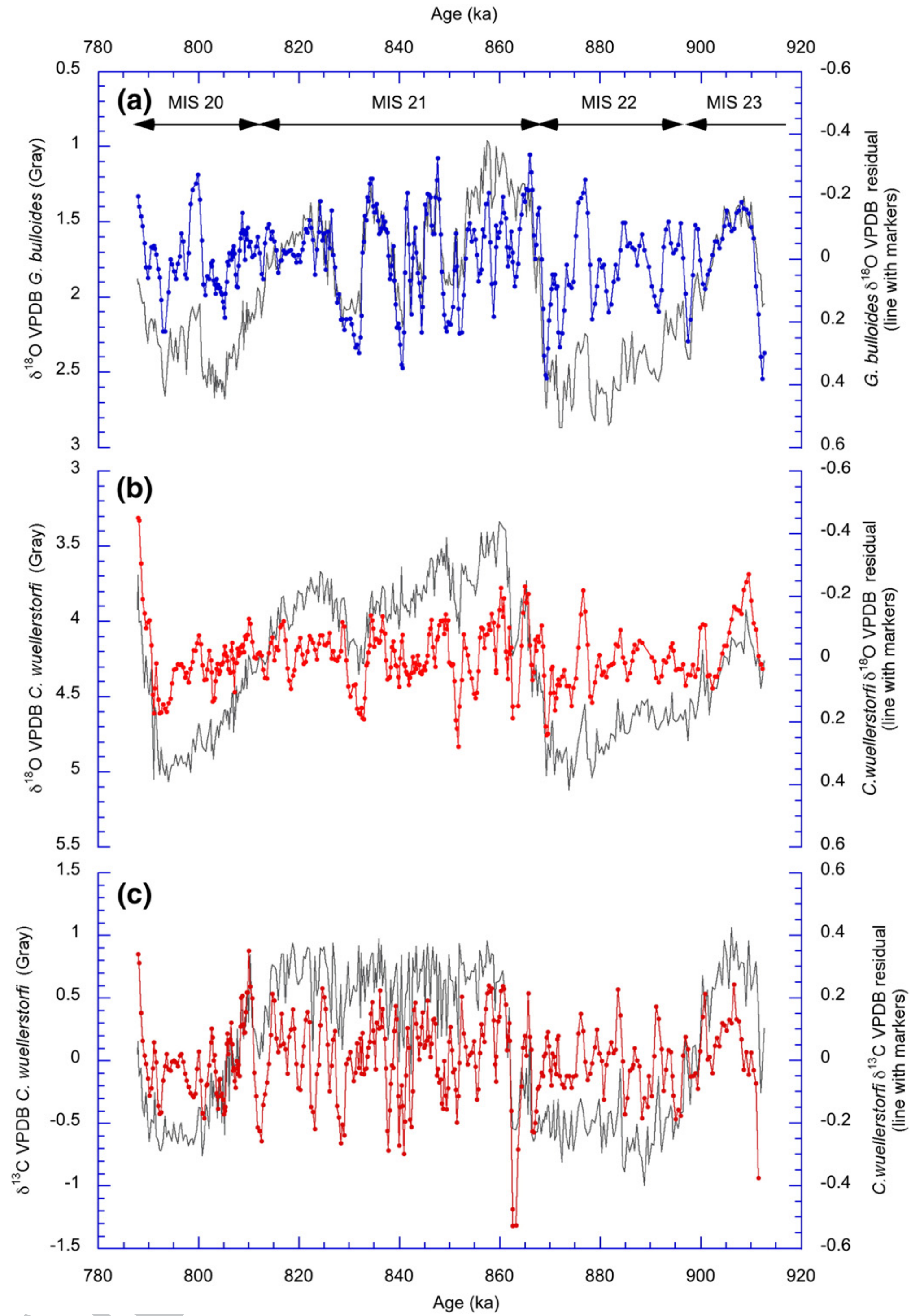


**Fig. 3.** The residual obtained by subtracting the Gaussian interpolation from the measured records of (a) *Globigerina bulloides* $\delta^{18}O$, (b) *Cibicidoides wuellerstorfi* $\delta^{18}O$, (c) *C. wuellerstorfi* $\delta^{13}C$ (thin lines with data point markers). The wide-Gaussian window (low periodicity) filtered data were linearly interpolated onto the age values of the original data in order to conserve the original variance of the data, and the difference obtained. Also shown are the three measured records (gray line without marker) for stratigraphic reference.

four isotopic interstadial periods (21.1, 21.3, 21.5 and 21.7 in Fig. 2), revealing an interval of unstable climate. A partitioning of MIS 21 has already been documented by other deep-sea records, but this stage has been controversial and has proved difficult to astronomically tune in earlier work. Ruddiman et al. (1986) compressed this stage into a single obliquity cycle in DSDP Site 607, whereas Hilgen (1991) interpreted it as containing two tilt cycles; on the other hand Bassinot et al. (1994) identified three peaks in core MD900963 from the tropical Indian Ocean, and interpreted them as related to precession cycles. Thus, from previous work, it seems that the length and number of the cycles over oxygen stage 21 may depend on the resolution of the record, the region and the climate proxy studied. The recognition of an apparent "extra" major climate cycle in the stable isotope records from Site U1313 raises questions about whether this feature has basin-wide chronostratigraphic implications or is driven by local processes. In order to test these hypotheses, we have compared the benthic stable isotope records from

Please cite this article as: Ferretti, P., et al., North Atlantic millennial-scale climate variability 910 to 790 ka and the role of the equatorial insolation forcing, Earth Planet. Sci. Lett. (2010), doi:10.1016/j.epsl.2010.02.016

ARTICLE IN PRESS



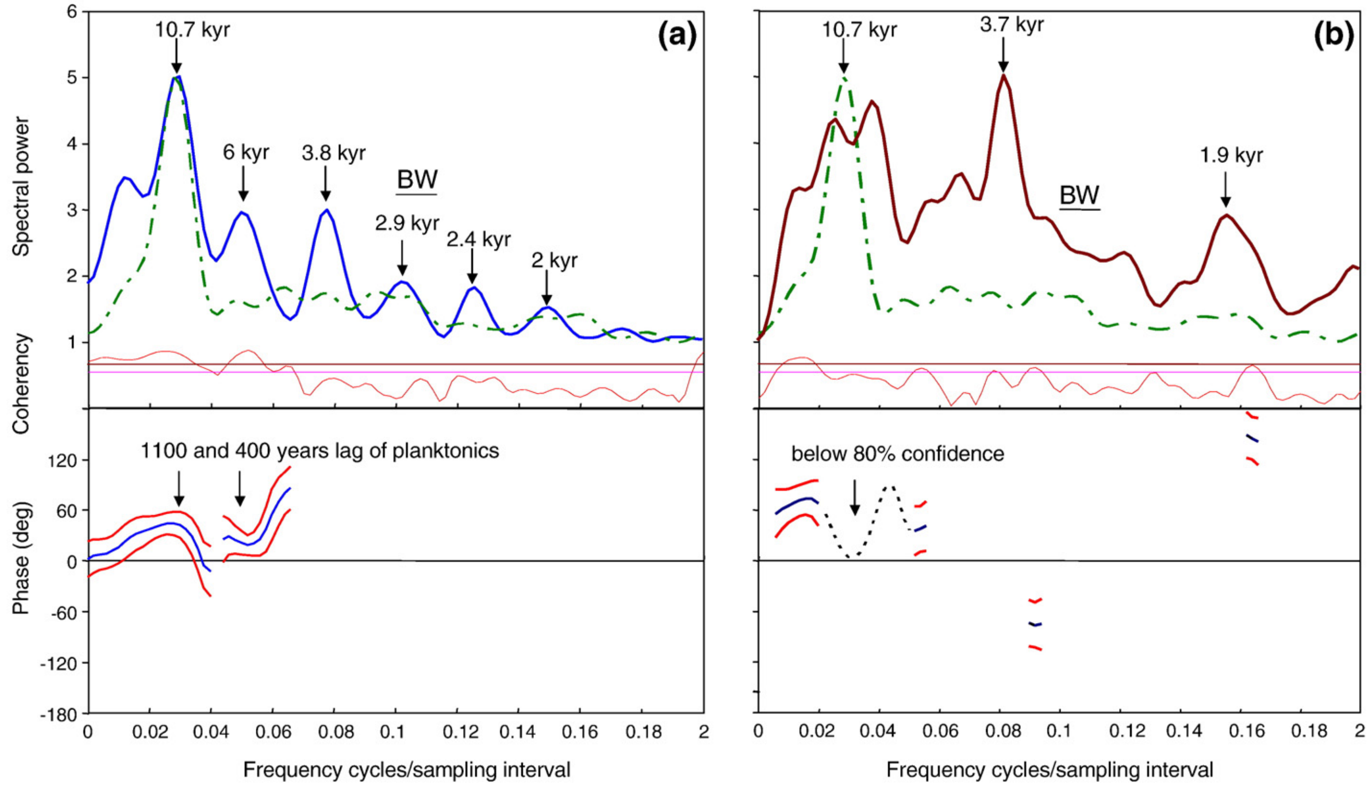


**Fig. 4.** Linear variance spectra obtained using Blackman–Tukey cross-spectral analysis. For spectral analysis, the residuals were interpolated to 0.3 kyr intervals using a 1 kyr Gaussian window. The top section shows the linear power spectrum, and the bottom shows phases for each coherent band, using the convention where phase angle is a measure of the lag (positive) or lead (negative) in degrees of the *Y* parameter with respect to the *X* parameter at any particular periodicity. (a) Cross-spectral analysis of the benthic $\delta^{18}O$ residual (*X* parameter, blue solid line) and planktonic $\delta^{18}O$ residual (*Y* parameter, green dashed line); (b) Cross-spectral analysis of the planktonic $\delta^{18}O$ residual (*X* parameter, green dashed line) and the benthic $\delta^{13}C$ residual (*Y* parameter, brown solid line). The dashed line in the phase plot indicates that the phase estimate is just below the 80% confidence criterion. The bar labelled BW indicates bandwidth. 80% and 95% confidence limits for coherency (horizontal lines) are also shown. Red lines in the phase plots indicate upper and lower error estimates. Brown University ARAND software was used for these analyses.

UNCORRECTED

Site U1313 with other detailed records from high-latitude and subtropical North Atlantic sites (Fig. 1).

Ocean Drilling Program (ODP) Site 983 is located on the Gardar drift, on the eastern flank of the Reykjanes ridge, at 1985 m water depth; during the last glacial maximum, this site was on the interface between Glacial North Atlantic Intermediate Water (GNAIW) and Southern Ocean Deep Waters in the North Atlantic (Oppo et al., 1997). Integrated Ocean Drilling Program Site U1308 is the reoccupation of Deep Sea Drilling Project Site 609. Located on the eastern side of the Mid-Atlantic Ridge at 3872 m water depth, this site is within the lower North Atlantic Deep Water (NADW) (Hodell et al., 2008); during the last glaciation, the site was more influenced by Lower Deep Water of Southern Ocean origin (Curry and Oppo, 2005). ODP Site 1063 is positioned on the sediment drift that constitutes the NE Bermuda Rise, in the northern Sargasso Sea; this site lies at 4584 m water depth, within the present mixing zone between the lower limb of NADW and Antarctic Bottom Water (AABW) (Keigwin et al., 1994). Together with Site U1313, these sites form a depth transect spanning the interval between ca. 2000 and 4500 m water depth in the North Atlantic, increasing the spatial data coverage within the North Atlantic.This transect encompasses the whole depth range of NADW masses during interglacial periods, including the shifts of GNAIW, NADW and AABW boundaries during glacial and unstable periods.

The benthic isotope records from Sites 983 (Kleiven et al., 2003), U1308 (Hodell et al., 2008), U1313 (this study) and 1063 (Ferretti et al., 2005) are plotted versus age in Fig. 5. A noticeable feature of this comparison is that each of the four peaks recorded at Site U1313 within MIS 21 has an equivalent at Sites 983, U1308 and 1063, confirming that these events were recorded at various depths and latitudes in the North Atlantic. This observation increases confidence in the interpretation of the benthic isotope variations as reflecting regional deep ocean circulation rather than being driven by local processes.

Within MIS 21, higher amplitude suborbital oscillations are observed in the oxygen isotope record at Site 983, resulting from a combination of lighter $\delta^{18}O$ values during warm episodes together with the persistence of nearly identical $\delta^{18}O$ values at the four sites during cold episodes. This different amplitude of the $\delta^{18}O$ signal indicates different temperature and local $\delta^{18}O$ signatures of deep-water bathing each site. Located in the shallower position in the depth transect, the $\delta^{18}O$ record at Site 983 reflects warmer intermediate source water, whereas Sites U1308/U1313 and 1063, respectively in the core of NADW and at the interface between NADW and AABW, are bathed by deeper water masses. However, considering that intermediate source waters bathing Site 983 are relatively cold today (Yashayaev et al., 2007), it is likely that temperature alone does not account for all of the benthic $\delta^{18}O$ offset observed (0.5‰) between the interglacial $\delta^{18}O$ values at Site 983 and the deeper sites, and salinity changes may have also played a role. In addition, the influence of isotopically light water from small melting episodes cannot be completely ruled out at the shallowest Site 983 (Dokken and Jansen, 1999; Kleiven et al., 2003). On the other hand, many of the foraminiferal $\delta^{18}O$ values at the Site 1063 are 0.2–0.3‰ lighter than those at the shallower Sites U1313 and U1308, possibly reflecting higher relative proportions of colder, low-$\delta^{18}O_{deepwater}$ AABW versus warmer, high- $\delta^{18}O_{deepwater}$ NADW at this deeper site.

The recognition of four mayor climatic cycles within MIS 21 has important implications not only in terms of oxygen isotope stratigraphy but also for the hydrographic and climatic interpretation of the benthic isotope signal, which provides evidence from the lower limb of the

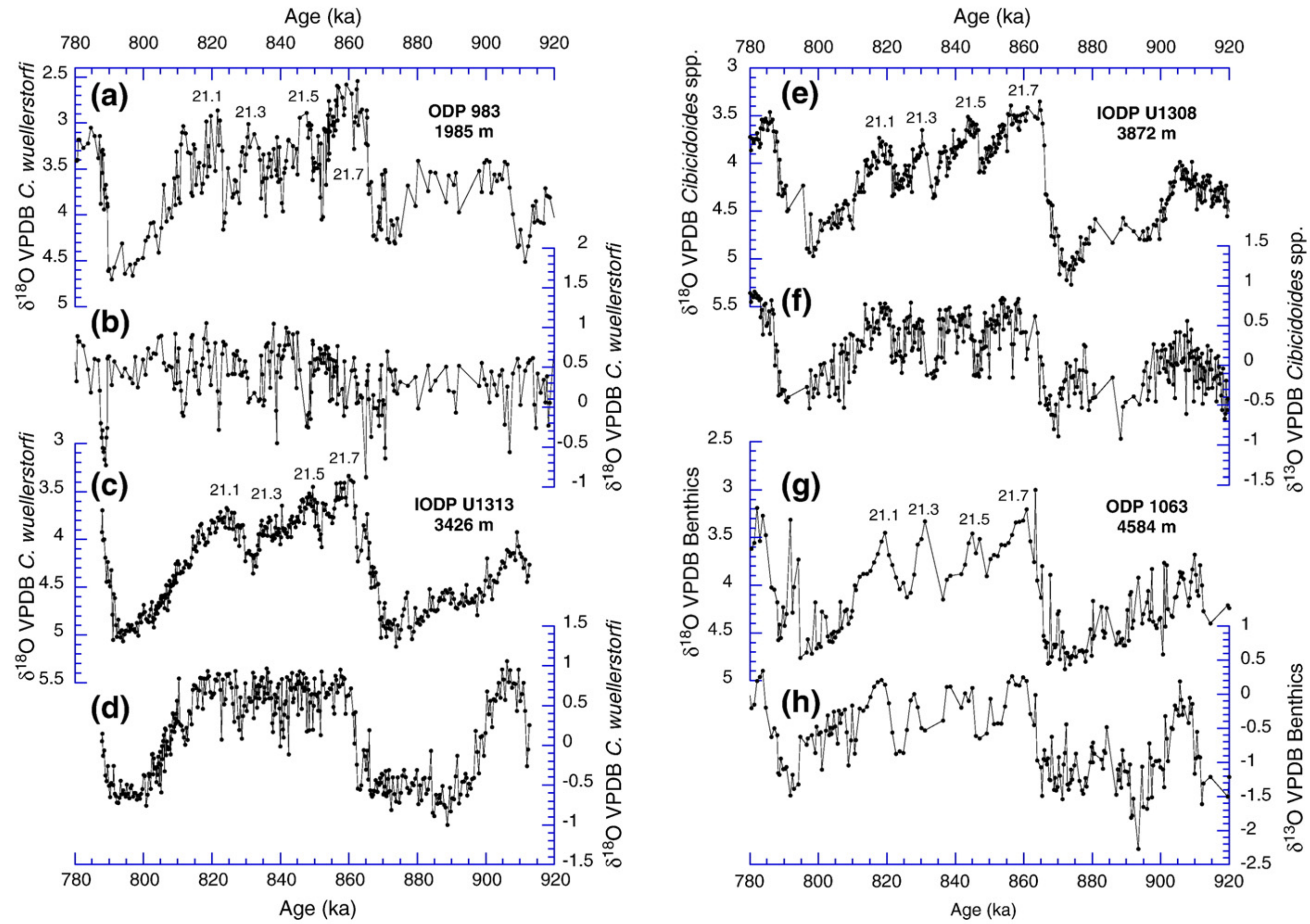


**Fig. 5.** Oxygen (a) and carbon (b) isotope records for benthic foraminifera *Cibicidoides wuellerstorfi* from ODP Site 983 (Kleiven et al., 2003). Oxygen (c) and carbon (d) isotope records for benthic foraminifera *C. wuellerstorfi* from IODP Site U1313 (this study). Oxygen (e) and carbon (f) isotope records for benthic foraminifera *C. wuellerstorfi* and *C. kullenbergi* from IODP Site U1308 (Hodell et al., 2008). Oxygen (g) and carbon (h) isotope records for benthic foraminifera from ODP Site 1063 (Ferretti et al., 2005). When necessary, isotope correction factors were used to adjust values for the various species analysed towards isotopic equilibrium values (for $^{18}$O) and towards an estimated $^{13}$C content of dissolved $CO_2$ (for $^{13}$C). All records are shown on their published age models, a part from those of ODP Site 983, which have been revised. Isotopic substages, as defined in this work, are also reported.

UNCORRECTED

Atlantic Meridional Overturning Circulation (AMOC). It is significant that these $\delta^{18}$O oscillations can be traced throughout the NADW depth range, implying that the different NADW source water masses and their relevant convection areas are similarly affected. Four peaks are also recorded in the benthic $\delta^{13}$C records at the three deeper sites, where much of the benthic $\delta^{13}$C variability can be ascribed primarily to changes in the relative strength of NADW versus AABW. At Site U1313, each low benthic $\delta^{13}$C event occurs during an interval of high planktonic $\delta^{18}$O (Fig. 2), implying that the ventilation of the North Atlantic was reduced during surface cold events and suggesting a coupling between surface temperature changes and the strength of the AMOC. Although speculative, these observations would be consistent with a southward extension of the subpolar gyre and thus a southward displacement and lower transport of the North Atlantic Drift. This would imply a reduction of the northward heat flux carried by the North Atlantic surface ocean into the deep-water convection areas. It is noteworthy that inputs of ice-rafted material, inferred from episodes of high content of magnetic particles, occurred in the Nordic Seas during MIS 21 (Helmke et al., 2005). Taken together, the evidence from the Nordic Seas and Site U1313 may support a link between iceberg discharge, increased freshening of the surface waters and reduced convection during MIS 21.

At Site U1313, episodes of weak NADW (inferred from low benthic $\delta^{13}$C values), associated with planktonic $\delta^{18}$O evidence for surface cooling mirror a pattern frequently described in late Pleistocene climate records; thus it seems that the glacial and orbital boundary conditions can vary considerably, while this coupling regularly persists.

### *4.2. Harmonics of precession imprints in the North Atlantic*

In order to explore the nature of the suborbital variability more closely, we have examined whether the climate variations observed during MIS 21 had a counterpart during glacial periods and extended our study to the whole interval, MIS 23–20. Suborbital variability is indeed recorded throughout the isotope records at Site U1313 and spectral analysis indicates significant variability is centred on periods of 10.7- and 6-kyr (Fig. 4). This timing is particularly interesting because it is close to peaks expected from the second and the fourth-harmonics of the precessional component of the insolation forcing.

In recent years, several studies have invoked or observed this type of response in nonlinear models of climate, in insolation records and in high-resolution records of climate variations. In modelling studies, two mechanisms are usually thought responsible for oscillations equal to the half-precessional signal. The first is that, in equatorial regions, the combination of the overhead passage of the Sun at either Equinox, together with perihelion, produces maximal temperatures; this phenomenon takes place twice during each precession cycle, and consequently generates a signal at near half the precession period (10 to 12 kyr) (Short et al., 1991). In this model, precession harmonics are primarily restricted to the equatorial regions, but it is feasible that this temperature response is exported into higher latitudes by tropical convective processes, either atmospheric or oceanic. Another way to produce semiprecession cycles is related to the alignment of each solstice with perihelion. Perihelion coincides only once with the Northern Hemisphere summer solstice during one precessional cycle. However, a Southern Hemisphere precession signal can be exported to the Northern Hemisphere and, because the two hemispheres are 180° out of phase in relation to precession, this would generate a semiprecession cycle in the Northern Hemisphere (Rutherford and D'Hondt, 2000).

Insolation records have predicted not only the existence of half-precession periods, but also the occurrence of the fourth-harmonics of precession cycles (11 kyr and 5.5 kyr respectively). These cycles have been identified in a calculation of the amplitude of the seasonal cycle of the energy that the equatorial (and to a lesser extent the intertropical) regions received from the Sun over the last 1 Ma (Berger et al., 2006). In line with the model proposed by Short et al. (1991), these cycles are clearly identified at the Equator; they are still present in the intertropical belt, but their amplitude decreases rapidly moving away from the Equator.

Other studies have specifically targeted past millennial-scale climate variability and identified 11 kyr cycles (Hagelberg et al., 1994; McIntyre and Molfino, 1996; Wara et al., 2000; Chaisson et al., 2002; Niemitz and Billups, 2005), and 5 kyr cycles in proxy records (Weirauch et al., 2008), so that there is now evidence for a climate system response to the harmonics of the precession band in geologic records from both low-

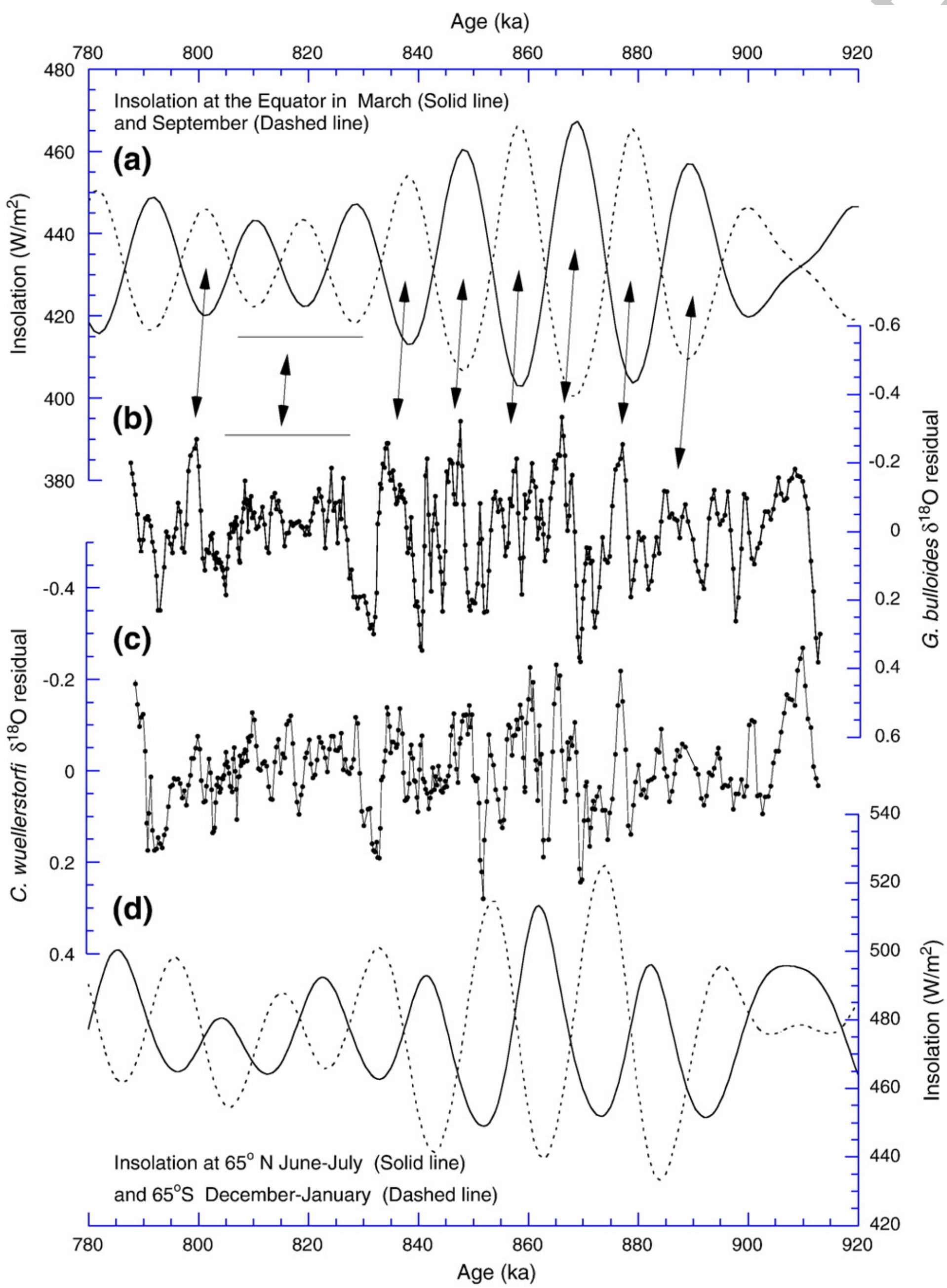


**Fig. 6.** Comparison of planktonic and benthic foraminiferal $\delta^{18}O$ residual from Site U1313 to different insolation records (Laskar et al., 2004): (a) the insolation at the Equator in Spring (solid line) and Autumn (dashed line); (b) the residual obtained by subtracting the Gaussian interpolation from the measured records of *Globigerina bulloides* $\delta^{18}O$; (c) the residual obtained by subtracting the Gaussian interpolation from the measured records of *Cibicidoides wuellerstorfi* $\delta^{18}O$; (d) Northern Hemisphere summer insolation (65°N, June–July) (solid line) and Southern Hemisphere summer insolation (65°S, December–January) (dashed line).

Please cite this article as: Ferretti, P., et al., North Atlantic millennial-scale climate variability 910 to 790 ka and the role of the equatorial insolation forcing, Earth Planet. Sci. Lett. (2010), doi:10.1016/j.epsl.2010.02.016

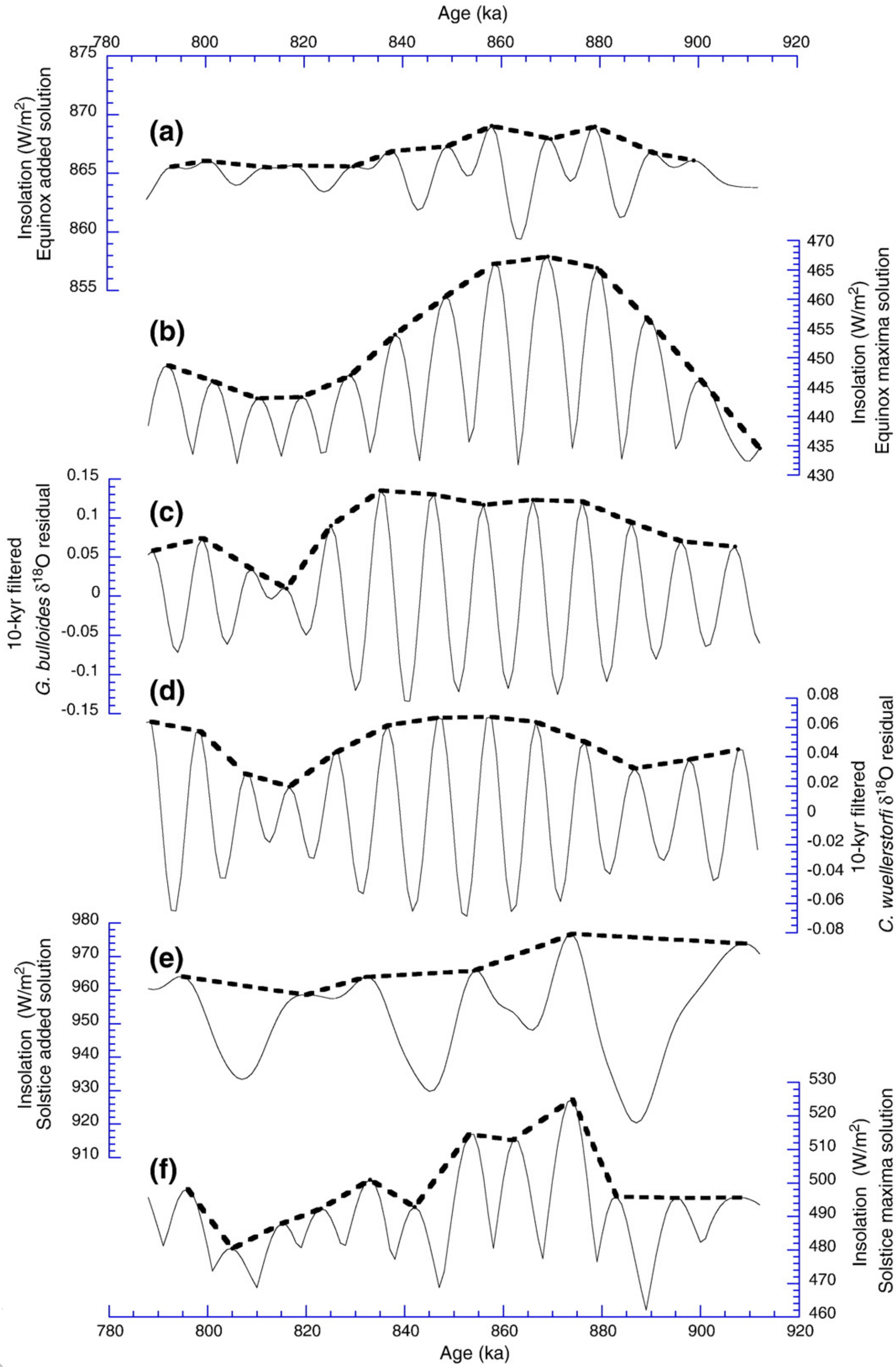


**Fig. 7.** Comparison of foraminiferal $\delta^{18}O$ residual from Site U1313 to different forcing models. Solid lines represent: (a) the "Equinox added" solution; (b) the "Equinox maxima" solution; (c) the 10-kyr Gaussian bandpass filter (0.1 central frequency, 0.02 width) of the planktonic foraminiferal $\delta^{18}O$ residual; (d) the 10-kyr Gaussian bandpass filter (0.1 central frequency, 0.02 width) of the benthic foraminiferal $\delta^{18}O$ residual; (e) the "Solstice added" solution; (f) the "Solstice maxima" solution. See text for an explanation about how the different orbital forcing models were obtained. Thick dashed lines represent the upper amplitude envelope of the variables.

and high-latitude locations. In most of these studies, the mechanism most frequently proposed to explain the half-precession signal involves the generation of half-precessional climate variability in the tropics, which is then advected to the high latitudes with relatively little lag.

Alternatively, a different scenario has been proposed to explain oscillations at frequencies equal to half-precession harmonics in the North Atlantic Ocean, which involves a regional response to high latitude orbital forcing (Wara et al., 2000).

Please cite this article as: Ferretti, P., et al., North Atlantic millennial-scale climate variability 910 to 790 ka and the role of the equatorial insolation forcing, Earth Planet. Sci. Lett. (2010), doi:10.1016/j.epsl.2010.02.016

ARTICLE IN PRESS



In order to resolve the driving mechanism of records observed at Site U1313 in the context of a low- or high-latitude climate forcing, we have compared them to different insolation records (Laskar et al., 2004): a) the insolation at the Equator in March and September (Fig. 6a), in order to test the hypothesis by Short et al. (1991) and b) the insolation at both 65°N in June–July and 65°S in December–January (Fig. 6d) to test the hypothesis by Rutherford and D'Hondt (2000).

There is substantial agreement between the benthic and planktonic $\delta^{18}O$ residual records and insolation at the Equator during the Equinoxes (Fig. 6a). The two oxygen isotope records not only follow the pattern but also mimic the amplitude of insolation. From ~880 to ~830 ka, *G. bulloides* and *C. wuellerstorfi* $\delta^{18}O$ values parallel the multiple, relatively high-amplitude insolation variations. The comparatively small insolation variations during the preceding and subsequent intervals are also apparent in the $\delta^{18}O$ records of *G. bulloides* and *C. wuellerstorfi*. The phase offset between the timing of changes in the insolation and the proxy records possibly reflects a delay in the response of the climate system to the astronomical forcing or could also be an artefact of the orbitally tuned age model. In contrast, the insolation at 65°N–S shows a very different evolution, both in terms of timing and amplitude variations, which does not correlate as closely to the climate signal at Site U1313 (Fig. 6d); these observations make control from those regions appear unlikely.

#### 4.2.1. Cross-correlation coefficients between the forcing and the climatic response

To evaluate the strength of the relationship between the amplitude modulation of the possible forcing and the proxy response, we have compared the amplitude envelopes of the 10 kyr-filtered foraminiferal $\delta^{18}O$ residuals with the two candidates for orbital forcing — Equinoxes at the Equator and Solstices at both 65°N and 65°S. To combine the elements of the forcing to a single line, we used two models: a) adding the total insolation curves (solutions called “Equinox added” and “Solstice added”), or b) combining them by using the maxima from either curve, (switching from one curve to another whenever the insolation in one curve exceeded that in the other), on the assumption that warming responses would be driven by the higher insolation (solutions called “Equinox maxima” and “Solstice maxima”) (Fig. 7). This second procedure generated forcing models with little amplitude variation on the lower part of the curve (minimum values). Cross-correlation coefficients were therefore examined on the upper amplitude envelopes of the variables only (Fig. 7). To make a comparison that was not biased by the absolute position of the cycles relative to the orbital forcing, the cross-correlation was lagged or led the response to the forcing by the equivalent of a precession cycle (i.e. 21-kyr steps) in case the assumptions about the phase relationship to precession had “misplaced” the subMilankovitch components in relation to the forcing. A good correlation at an extreme lead or lag in relation to the existing age model would be suspect on chronostratigraphic grounds.

Cross-correlation shows consistently better correlation coefficients for Equinox-based solutions rather than Solstice forcing models (Fig. 8). The mean of the planktonic and benthic correlation coefficients at each of the offsets to the forcing shows that the highest value obtained for the Equinox models is 0.79 at 7 kyr lag with respect to the orbital forcing models (for the Equinox maxima solution), and for the Solstice models is 0.69 at zero lag (for the Solstice maxima solution). The better predictions based on equinoctial forcing are due to the presence of a greater influence of orbital obliquity on the Solstice curves; in contrast, the effect of the obliquity component of the high-latitude forcing is virtually absent in the low-latitude forcing (Fig. 9). These results indicate that the equinoctial forcing is a better fit to the proxy data. They do not preclude the possibility that high-latitude forcing is responsible for the observed response, but they do suggest that low-latitude forcing provides a more complete and effective explanation for it.

#### 4.2.2. Transport of the equatorial signal to the higher latitudes

The very good match between the proxy records and the insolation at the Equator supports the hypothesis that forcing from low latitudes might be implicated in the origin of the harmonics of precession cycles observed at Site U1313. This is in agreement with recent insolation records showing that maximum and minimum equatorial insolation have pronounced precession harmonics, mainly 11 kyr (Berger et al., 2006; Ashkenazy and Gildor, 2008) and 5 kyr (Berger et al., 2006). In addition, a driving mechanism based on low-latitude insolation would be consistent with the observation that the higher amplitude variations at Site U1313 are mainly concentrated between ~880 and ~830 ka, an interval which includes the MIS 22–21 transition and most of MIS 21. Such a mechanism would be working continuously throughout glacial–interglacial cycles, explaining why no obvious ice volume threshold seems important for setting the stage for high-amplitude variability at our site.

In order to influence climate variability at Site U1313, energy would have to be transported into high latitudes away from equatorial regions. Modelling studies suggest that atmospheric and oceanic circulation could reasonably be invoked to transmit the equatorial response to the high latitudes (Short et al., 1991). At DSDP Site 607 from the same location (Site U1313 was a reoccupation of Site 607), the relative abundance of the coccolithophorid *Florisphaera profunda* presents high-amplitude, short-term shifts from MIS 23 to the MIS 22/21 transition, when a rapid decrease starts to be recorded (Marino et al., 2008). This species is restricted to the lower part of the euphotic zone (Okada and Honjo, 1973) and has been used as an indicator of the depth of the nutricline (Molfino and McIntyre, 1990a,b; McIntyre and Molfino, 1996). The relative abundance of *F. profunda* increases when the upper photic zone is impoverished in nutrients and the nutricline deepens; in contrast, its abundance decreases when wind stress generates a rise of the nutricline and an increase of primary production in the upper photic zone. Present-day satellite observations indicate that in the North

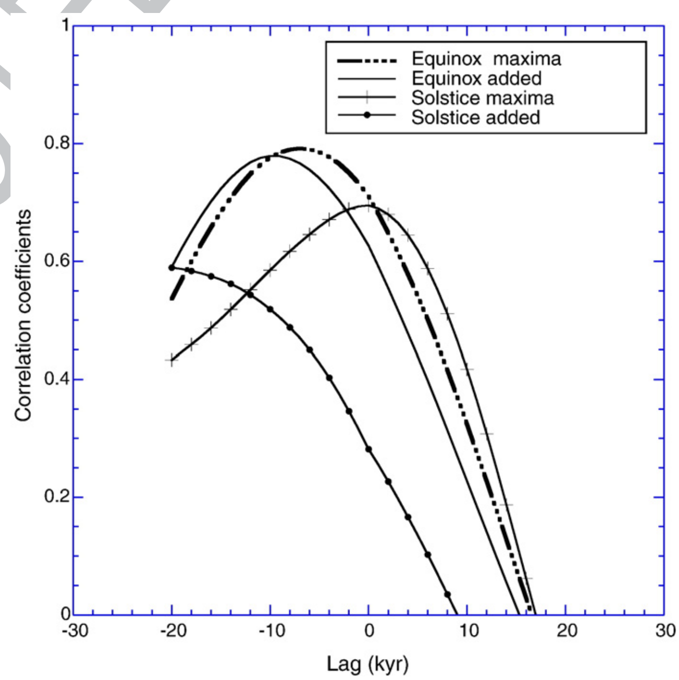


**Fig. 8.** Cross-correlation coefficients for the upper amplitude envelopes of the 10-kyr-filtered planktonic and benthic foraminiferal $\delta^{18}O$ residual versus the upper amplitude envelopes of the Equinox (“Equinox added” solution = solid line; “Equinox maxima” solution = dashed line) and Solstice forcings (“Solstice added” solution = line with solid dots; “Solstice maxima” solution = line with crosses). The values represented here were obtained by taking the mean of the two planktonic and benthic correlation coefficients versus the orbital forcing models at each of the offsets to the forcing. Negative values on the *X* axis correspond to a lag of the climatic response with respect to the orbital forcing. The cross-correlations suggest a lag of mean climatic response to the orbital forcing “Equinox maxima” solution of about 7 kyr relative to the timescale presented here. No optimal lag is attained for the “Solstice max” solution.

UNCORRECTED PROOF

Please cite this article as: Ferretti, P., et al., North Atlantic millennial-scale climate variability 910 to 790 ka and the role of the equatorial insolation forcing, Earth Planet. Sci. Lett. (2010), doi:10.1016/j.epsl.2010.02.016

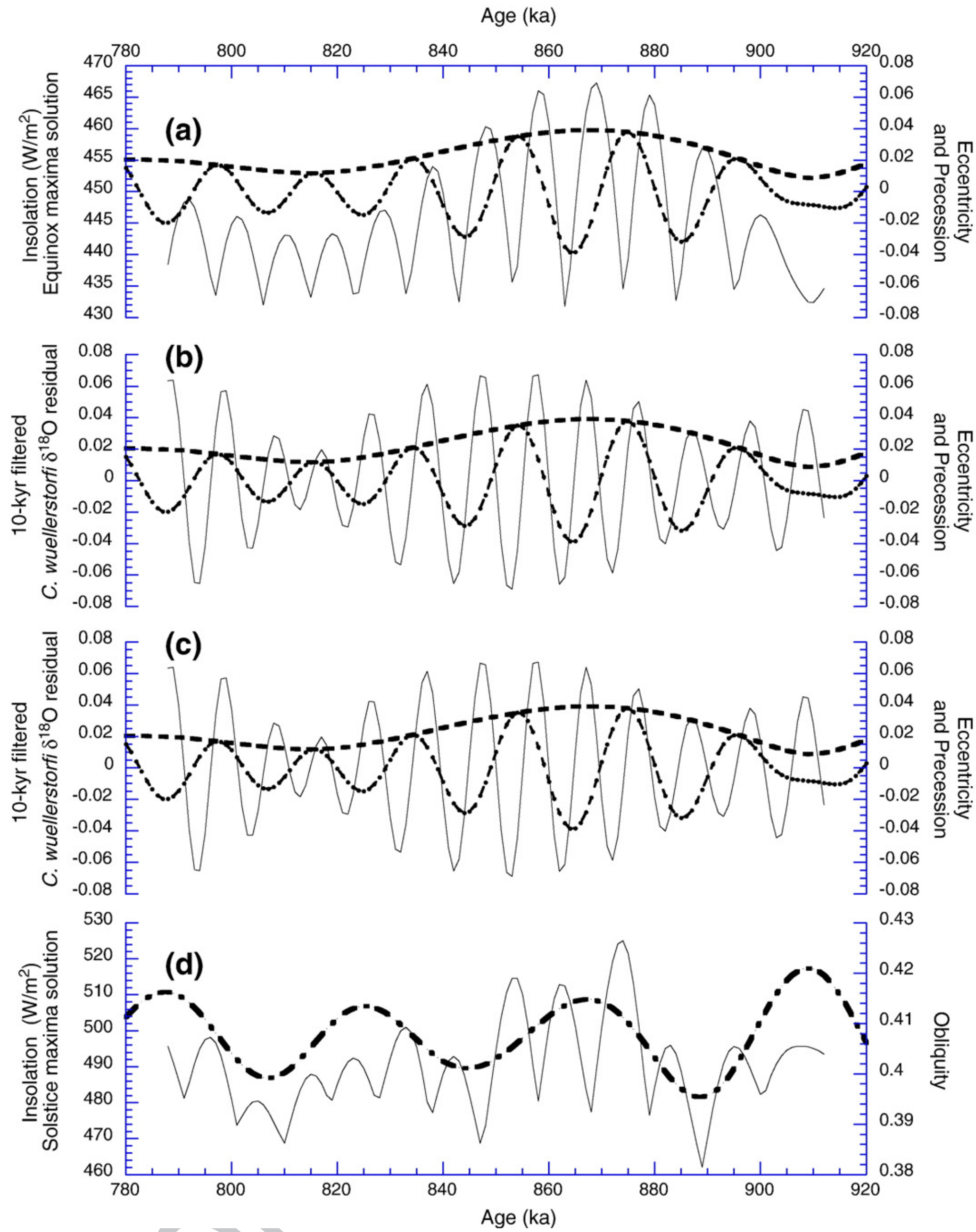


**Fig. 9.** Comparison of foraminiferal $\delta^{18}O$ residual from Site U1313 and forcing models to the Earth's orbital parameters (Laskar et al., 2004). (a) the "Equinox maxima" solution (solid line) together with orbital eccentricity (dashed line) and precession (dashed line with cycles); (b) the 10-kyr Gaussian band filter of the planktonic foraminiferal $\delta^{18}O$ residual (solid line), orbital eccentricity (dashed line) and precession (dashed line with cycles); (c) the 10-kyr Gaussian band filter of the benthic foraminiferal $\delta^{18}O$ residual (solid line), orbital eccentricity (dashed line) and precession (dashed line with cycles); (d) the "Solstice maxima" solution (solid line) together with obliquity (dashed line).

Atlantic high winds occur mainly over the open ocean where the northward flowing Gulf Stream leaves the Grand Banks and retroflects into the broad eastward North Atlantic Current (Sampe and Xie, 2007), very close to the location of Site U1313. If the abundance fluctuations of *F. profunda* at Site 607 prove to reflect changes in the nutricline position related to a strengthening of atmospheric surface winds, then it appears that very dynamic oceanic/atmospheric conditions characterized this area during the time interval considered in this study. Stronger atmospheric winds were hypothesized by Weirauch et al. (2008) after MIS 22, when an increase in ice volume induced stronger pole-to-equator temperature gradients.

Increased poleward flow of surface westerlies directly affects the displacement of warm tropical waters towards the high latitudes in the North Atlantic by the Gulf Stream and North Atlantic Drift, and it is conceivable that this process could have contributed to export the equatorial temperature response to the higher latitudes.

### 4.3. Phase relationship between surface and deep-water records

At Site U1313, we observe a phase difference between the oxygen isotope records of *C. wuellerstorfi* and *G. bulloides*, with the benthic $\delta^{18}O$ leading the planktonic $\delta^{18}O$ by 1100 years in the 10.7 kyr band and by 400 years in the 6 kyr band (Fig. 4a). At DSDP Site 607, sea surface temperature lags 3000 years behind the benthic $\delta^{18}O$ in the 23 kyr band, confirming a phase lead of the deep-water signal over the surface record even at orbital timescales (Ruddiman et al., 1989). Asynchrony between

Please cite this article as: Ferretti, P., et al., North Atlantic millennial-scale climate variability 910 to 790 ka and the role of the equatorial insolation forcing, Earth Planet. Sci. Lett. (2010), doi:10.1016/j.epsl.2010.02.016

benthic and planktonic foraminiferal $\delta^{18}O$ records has already been observed in sediment cores from the Northern (Shackleton et al., 2000) and Southern Hemispheres (Charles et al., 1996). Although the phase relationship between proxies from a single core is relatively incontrovertible, a straightforward interpretation of this phase offset is not yet available.

Some of the features in the oxygen records at Site U1313 partly resemble the pattern described for the Northeast Atlantic, where the benthic $\delta^{18}O$ was originally interpreted as providing evidence of changes in continental ice volume (Shackleton et al., 2000). For example, at around 848 ka, the benthic $\delta^{18}O$ enrichment began when the planktonic $\delta^{18}O$ values were still close to their lightest value (Fig. 2). Warm sea surface temperatures, as inferred from the planktonic $\delta^{18}O$, create optimal conditions for rapid continental ice growth by providing moisture, due to the large temperature gradients between the atmosphere and the ocean. On orbital timescales, Ruddiman and McIntyre (1979, 1981) depicted a similar scenario using sea surface temperature (SST) data from the northwestern subtropical gyre and the subpolar ocean, which maintained relatively warm SSTs during the rapid ice growth phases of the last 250,000 years and acted primarily as a moisture amplifier of continental ice-sheet growth and decay at the 23 kyr period. At around 852 ka, the benthic $\delta^{18}O$ depletion starts before the planktonic oxygen isotope signal reaches its heaviest values; when the surface of the North Atlantic was cold, local moisture supply and possibly influx of low-latitude moisture were suppressed, inducing ice decay. It is interesting to note that in the process of picking foraminifera for geochemical analyses, at ca. 852 ka we found traces of mineral grains (>150 microns, mostly quartz), which were probably recording the episodic input of ice-rafted detritus to Site U1313.

However, this interpretation is not entirely free of complications because the North Atlantic is sensitive to rapid exchanges between different deep-water masses with contrasting $\delta^{18}O$ and temperature signatures (Skinner et al., 2003). For this reason, variations in the benthic $\delta^{18}O$ at Site U1313 may reflect not only fluctuations in ice volume during millennial events but also local changes in deep-water hydrography associated with AMOC perturbations. Benthic $\delta^{13}C$ at this site is a good indicator of AMOC changes (Raymo et al., 1990, 2004), and the observation that this signal lags the benthic $\delta^{18}O$ in the above mentioned interval (852–848 ka) provides support to the hypothesis that some of the major transitions in the benthic $\delta^{18}O$ record appear to be controlled generally, though not exclusively, by ice volume changes. It is not very straightforward to extend this line of reasoning to the whole interval of time analysed in this study, because the phasing of some of the climate variables remain to be determined precisely and does not provide information about the causal relationships. In particular, the absolute spectral peaks in the benthic $\delta^{13}C$ residual do not occur at the same periods as the benthic and planktonic $\delta^{18}O$ residuals (Fig. 4); moreover, the lack of significant coherency between the benthic $\delta^{13}C$ and planktonic $\delta^{18}O$ residuals (Fig. 4b) preclude a meaningful evaluation of the phase evolution in the interval analysed. On this basis, these observations would be more consistent with previous findings suggesting that both mechanisms–ice volume changes in the Northern Hemisphere ice sheets and hydrographic changes in deep water–could act together to cause the variability observed in the benthic oxygen isotope record at Site U1313.

We are aware that the ultimate mechanism behind this pattern remains equivocal in the absence of additional constraints on the significance of the benthic $\delta^{18}O$ record. In a more conservative way, we suggest that our results support an asynchronous relationship between surface and deep-water hydrography in the mid-latitude North Atlantic during MIS 23–20. The persistence of this pattern of response during different glacial and orbital boundary conditions in the Pleistocene indicates that this is a robust feature of the climate system and an important consideration of any theory of orbital and millennial-scale climate change.

## 5. Conclusions

Stable isotope records from IODP Site U1313, in the mid-latitude North Atlantic, document a detailed history of surface conditions and their relationship to regional and deep-water changes over the interval 910–790 ka (from late in MIS 23 to MIS 20).

During interglacial MIS 21, four major climate cycles have been identified and correlated across the North Atlantic Ocean. These events occurred more frequently than can be explained by a linear response to cyclical changes in orbital geometry, as suggested in previous work. Surface cold events co-existed with relatively poorly ventilated deep waters, implying that changes in the Atlantic meridional overturning circulation were implicated in these events.

Time series analyses indicate that the benthic and planktonic oxygen isotope records contain significant millennial-scale variability at periods of 10.7 and 6 kyr, which correspond to harmonics of the precession cycles, and these cycles can be observed throughout this interval. A match with Spring and Autumn orbital forcing at low latitudes suggests that the source of this part of the climate signal at our Site is low-latitude insolation, with the equatorial response being advected to the high latitudes through oceanic and atmospheric circulation, after being possibly amplified by moisture feedback. Our results appear to support an asynchronous relationship between surface and deep-water records, in analogy with late Pleistocene climate records and confirming a pattern already identified at the same site on orbital timescales. While the regional extent of these events needs to be verified by future work, we suggest that the 10.7- and 6-kyr cycles recorded at Site U1313 provide support for a linked atmosphere–ocean–cryosphere system controlled by low latitude insolation forcing at these periodicities.

## Acknowledgements

We are especially indebted to James Rolfe for his care of the mass spectrometer and its operation. We are grateful to David Hodell and Kikki Kleiven for providing their isotope data, and Matteo Massironi, José-Abel Flores and Francisco Sierro for advice and discussions. We thank three reviewers, whose comments helped us to clarify our argument. Thanks to the scientific party of Expedition 306, to all crew members and IODP technical staff of the JOIDES Resolution for a productive cruise. This research used samples provided by the Integrated Ocean Drilling Program (IODP). Support from NERC (NE/D521530/1) and the European Union through a Marie Curie fellowship (to PF) is gratefully acknowledged. We would like to dedicate this manuscript to our friend and colleague Nick Shackleton, who worked with us during the early stages of this project, and whom we will never forget.

## References

Alley, R.B., 2007. Wally was right: predictive ability of the North Atlantic "Conveyor belt" hypothesis for abrupt climate change. Annu. Rev. Earth Planet. Sci. 35, 241–272.
Alley, R.B., Clark, P.U., Keigwin, L.D., Webb, R.S., 1999. Making sense of millennial-scale climate change. In: Clark, P.U., Webb, R.S., Keigwin, L.D. (Eds.), Mechanisms of Global Climate Change at Millennial Time Scale 112. American Geophysical Union, Washington, DC, pp. 385–394.
Ashkenazy, Y., Gildor, H., 2008. Timing and significance of maximum and minimum equatorial insolation. Paleoceanography 23, PA1206 doi:1210.1029/2007PA001436. Q2
Barendregt, R.W., Irving, E., 1998. Changes in the extent of North American ice sheets during the late Cenozoic. Can. J. Earth Sci. 35, 504–509.
Bassinot, F.C., Labeyrie, L.D., Vincent, E., Quidelleur, X., Shackleton, N.J., Lancelot, Y., 1994. The astronomical theory of climate and the age of the Brunhes–Matuyama magnetic reversal. Earth Planet. Sci. Lett. 126, 91–108.
Be', A.W.H., 1977. An ecological, zoogeographic and taxonomic review of recent planktonic foraminifera. In: Ramsay, A.T.S. (Ed.), Oceanic Micropaleontology 1. Academic Press, London, pp. 1–100.
Belanger, P.E., Curry, W.B., Matthews, R.K., 1981. Core-top evaluation of benthic foraminiferal isotopic ratios for paleo-oceanographic interpretations. Palaeogeogr. Palaeoclimatol. Palaeoecol. 33, 205–220.
Berger, A., Loutre, M.F., Melice, J.L., 2006. Equatorial insolation: from precession harmonics to eccentricity frequencies. Clim. Past 2, 131–136.

UNCORRECTED PROOF

Please cite this article as: Ferretti, P., et al., North Atlantic millennial-scale climate variability 910 to 790 ka and the role of the equatorial insolation forcing, Earth Planet. Sci. Lett. (2010), doi:10.1016/j.epsl.2010.02.016

Chaisson, W.P., Poli, M.-S., Thunell, R.C., 2002. Gulf Stream and Western Boundary Undercurrent variations during MIS 10–12 at Site 1056, Blake-Bahama Outer Ridge. Mar. Geol. 189, 79–105.

Chapman, M.R., Shackleton, N.J., 1998. Millennial-scale fluctuations in North Atlantic heat flux during the last 150,000 years. Earth Planet. Sci. Lett. 159, 57–70.

Chapman, M.R., Shackleton, N.J., 1999. Global ice-volume fluctuations, North Atlantic ice-rafting events, and deep-ocean circulation changes between 130 and 70 ka. Geology 27, 795–798.

Charles, C.D., Lynch-Stieglitz, J., Ninnemann, U.S., Fairbanks, R.G., 1996. Climate connections between the hemisphere revealed by deep sea sediment core/ice core correlations. Earth Planet. Sci. Lett. 142, 19–27.

Clark, P.U., Archer, D., Pollard, D., Blum, J.D., Rial, J.A., Brovkin, V., Mix, A.C., Pisias, N.G., Roy, M., 2006. The middle Pleistocene transition: characteristics, mechanisms, and implications for long-term changes in atmospheric $pCO_2$. Quatern. Sci. Rev. 25, 3150–3184.

Coplen, T.B., 1995. New IUPAC guidelines for the reporting of stable hydrogen, carbon, and oxygen isotope-ratio data. J. Res. Nat. Inst. Stand. Technol. 100, 285.

Curry, W.B., Oppo, D.W., 2005. Glacial water mass geometry and the distribution of δ13C of ΣCO2 in the western Atlantic Ocean. Paleoceanography 20, PA1017
Q3 doi:1010.1029/2004PA001021.

Dodonov, A.E., 2005. In: Head, M.J., Gibbard, P.L. (Eds.), The stratigraphic transition and suggested boundary between the Early and Middle Pleistocene in the loess record of Northern Eurasia. : Early–Middle Pleistocene Transitions: The Land Ocean Evidence, 247. he Geological Society, London, pp. 209–219.

Dokken, T.M., Jansen, E., 1999. Rapid changes in the mechanism of ocean convection during the last glacial period. Nature 401, 458–461.

Expedition 306 Scientists, 2006. In: Channell, J.E.T., Kanamatsu, T., Sato, T., Stein, R., Alvarez Zarikian, C.A., Malone, M.J., Scientists, A.T.E. (Eds.), Site U1313. : Proc. IODP, 306. Integrated Ocean Drilling Program Management International, Inc, College Station TX.

Ferretti, P., Shackleton, N.J., Rio, D., Hall, M.A., 2005. In: Head, M.J., Gibbard, P.L. (Eds.), Early–Middle Pleistocene deep circulation in the western subtropical Atlantic: Southern Hemisphere modulation of the North Atlantic Ocean. : Early–Middle Pleistocene Transitions: The Land Ocean Evidence, 247. The Geological Society, London, pp. 131–145.

Fratantoni, D.M., 2001. North Atlantic surface circulation during the 1990's observed with satellite-tracked drifters. J. Geophys. Res. 106, 22067–22093.

Hagelberg, T., Bond, G., De Menocal, P., 1994. Milankovitch band focing of sub-Milankovitch climate variability during the Pleistocene. Paleoceanography 9, 545–558.

Helmke, J.P., Bauch, H.A., Röhl, U., Mazaud, A., 2005. Changes in sedimentation patterns of the Nordic sea region across the mid-Pleistocene. Mar. Geol. 215, 107–122.

Heslop, D., Dekkers, M.J., Langereis, C.G., 2002. Timing and structure of the mid-Pleistocene transition: records from loess deposits of Northern China. Palaeogeogr. Palaeoclimatol. Palaeoecol. 185, 133–143.

Hilgen, F.J., 1991. Astronomical calibration of Gauss to Matuyama sapropels in the Mediterranean and implication for the geomagnetic polarity timescale. Earth Planet. Sci. Lett. 104, 226–244.

Hodell, D.A., Venz, K.A., Charles, C.D., Ninnemann, U.S., 2003. Pleistocene vertical carbon isotope and carbonate gradients in the South Atlantic sector of the Southern Ocean.
Q4 Geochem. Geophys. Geosyst. 4, 1004 doi:1010.1029/2002GC000367.

Hodell, D.A., Channell, J.E.T., Curtis, J.H., Romero, O.E., Rohl, U., 2008. Onset of "Hudson Strait" Heinrich events in the eastern North Atlantic at the end of the middle Pleistocene
Q5 transition (~640 ka)? Paleoceanography 23, PA4218 doi:4210.1029/2008PA001591.

Howell, P., Pisias, N.J., Ballance, J., Baughman, J., Ochs, L., 2006. ARAND Time-Series Analysis Software. Brown University, Providence RI. Available at http://www.ncdc.noaa.gov/paleo/softlib/arand/arand.html.

Imbrie, J., Berger, A., Boyle, E.A., Clemens, S.C., Duffy, A., Howard, W.R., Kukla, G., Kutzbach, J., Martinson, D.G., McIntyre, A., Mix, A.C., Molfino, B., Morley, J.J., Peterson, L.C., Pisias, N.G., Prell, W.L., Raymo, M.E., Shackleton, N.J., Toggweiler, J.R., 1993. On the structure and origin of major glaciation cycles. 2. The 100,000-year cycle. Paleoceanography 8, 699–735.

Jenkins, G.M., Watts, D.G., 1968. Spectral Analysis and Its Applications. Holden-Day, San Francisco. 525 pp.

Keigwin, L.D., Boyle, E.A., 1999. Surface and deep ocean variability in the northern Sargasso Sea during marine isotope stage 3. Paleoceanography 14, 164–170.

Keigwin, L.D., Curry, W.B., Lehman, S.J., Johnsen, S., 1994. The role of the deep ocean in North Atlantic climate change between 70 and 130 kyr ago. Nature 371, 323–326.

Kitamura, A., Kawagoe, T., 2006. Eustatic sea-level change at the Mid-Pleistocene climate transition: new evidence from the shallow-marine sediment record of Japan. Quatern. Sci. Rev. 25, 323–335.

Kleiven, H.F., Jansen, E., Curry, W.B., Hodell, D.A., Venz, K.A., 2003. Atlantic Ocean thermohaline circulation changes on orbital to suborbital timescales during the
Q6 mid-Pleistocene. Paleoceanography 18, 1008 doi:1010.1029/2001PA000629.

Laskar, J., Robutel, P., Joutel, F., Gastineau, M., Correia, A.C.M., Levrard, B., 2004. A long-term numerical solution for the insolation quantities of the Earth. A & A 428,
Q7 261–285 doi:210.1051/0004-6361:20041335.

Lisiecki, L.E., Raymo, M.E., 2005. A Pliocene–Pleistocene stack of 57 globally distributed
Q8 benthic δ18O records. Paleoceanography 20, PA1003 doi:1010.1029/2004PA001071.

Marino, M., Maiorano, P., Lirer, F., 2008. Changes in calcareous nannofossil assemblages during the Mid-Pleistocene revolution. Mar. Micropaleontol. 69, 70–90.

McClymont, E.L., Rosell-Mele´, A., 2005. Links between the onset of modern Walker circulation and the mid-Pleistocene climate transition. Geology 33, 389–392.

McIntyre, A., Molfino, B., 1996. Forcing of Atlantic equatorial and subpolar millennial cycles by precession. Science 274, 1867–1870.

Molfino, B., McIntyre, A., 1990a. Forcing of nutricline dynamics in the Equatorial Atlantic. Science 249, 766–769.

Molfino, B., McIntyre, A., 1990b. Nutricline variation in equatorial Atlantic coincident with the Younger Dryas. Paleoceanography 5, 997–1008.

Mudelsee, M., Schulz, M., 1997. The Mid-Pleistocene climate transition; onset of 100 ka cycle lags ice volume build-up by 280 ka. Earth Planet. Sci. Lett. 151, 117–123.

Muttoni, G., Carcano, C., Garzanti, E., Ghielmi, M., Piccin, A., Pini, R., Rogledi, S., Sciunnach, D., 2003. Onset of major Pleistocene glaciations in the Alps. Geology 31, 989–992.

Muttoni, G., Ravazzi, C., Breda, M., Pini, R., Laj, C., Kissel, K., Mazaud, K., Garzanti, E., 2007. Magnetostratigraphic dating of an intensification of glacial activity in the southern Italian Alps during Marine Isotope Stage 22. Quatern. Res. 67, 161–173.

Niemitz, M.D., Billups, K., 2005. Millennial-scale variability in western tropical Atlantic surface ocean hydrography during the early Pliocene. Mar. Micropaleontol. 54, 155–166.

Okada, H., Honjo, S., 1973. The distribution of oceanic coccolithophorids in the Pacific. Deep-Sea Res. 20, 355–374.

Oppo, D.W., Horowitz, M., Lehman, S.J., 1997. Marine core evidence for reduced deep water production during Termination II followed by a relatively stable substage 5e (Eemian). Paleoceanography 12, 51–63.

Oppo, D.W., McManus, J.F., Cullen, J.L., 1998. Abrupt climate events 500,000 to 340,000 years ago: evidence from subpolar North Atlantic sediments. Science 279, 1335–1338.

Oppo, D.W., Keigwin, L.D., McManus, J.F., 2001. Persistent suborbital climate variability in marine isotope stage 5 and Termination II. Paleoceanography 16, 280–292.

Paillard, D.L., Labeyrie, L., Yiou, P., 1996. Macintosh program performs time-series analysis. Eos Trans. Am. Geophys. Union 77, 379.

Pisias, N.G., Moore, T.C., 1981. The evolution of Pleistocene climate: a time series approach. Earth Planet. Sci. Lett. 52, 450–458.

Raymo, M.E., Ruddiman, W.F., Backman, J., Clement, B.M., Martinson, D.G., 1989. Late Pliocene variation in Northern Hemisphere ice sheets and North Atlantic Deep Water circulation. Paleoceanography 4, 413–446.

Raymo, M.E., Ruddiman, W.F., Shackleton, N.J., Oppo, D.W., 1990. Evolution of Atlantic–Pacific $\delta^{13}C$ gradients over the last 2.5 m.y. Earth Planet. Sci. Lett. 97, 353–368.

Raymo, M.E., Oppo, D.W., Flower, B.P., Hodell, D.A., McManus, J.F., Venz, K.A., Kleiven, K. F., McIntyre, K., 2004. Stability of North Atlantic water masses in face of pronounced climate variability during the Pleistocene. Paleoceanography 19, PA2008 doi:2010.1029/2003PA000921. Q9

Reverdin, G., Niiler, P.P., Valdimarsson, H., 2003. North Atlantic Ocean surface currents. J. Geophys. Res. 108, 3002 doi:3010.1029/2001JC001020. Q10

Ruddiman, W.F., McIntyre, A., 1979. Warmth of the Subpolar North Atlantic Ocean during Northern Hemisphere ice-sheet growth. Science 204, 173–175.

Ruddiman, W.F., McIntyre, A., 1981. Mechanisms for amplifications of the 23,000-year ice-volume cycle. Science 212.

Ruddiman, W.F., Raymo, M., McIntyre, A., 1986. Matuyama 41,000-year cycles: North Atlantic Ocean and Northern Hemisphere ice sheets. Earth Planet. Sci. Lett. 80, 117–129.

Ruddiman, W.F., Raymo, M.E., Martinson, D.G., Clement, B.M., Backman, J., 1989. Pleistocene evolution: Northern Hemisphere ice sheets and North Atlantic Ocean. Paleoceanography 4, 353–412.

Rutherford, S., D'Hondt, S., 2000. Early onset and tropical forcing of 100,000-year Pleistocene glacial cycles. Nature 408, 72–75.

Sampe, T., Xie, S.-P., 2007. Mapping high sea winds from space. A global climatology. Bull. Am. Meteorol. Soc. 1965–1978.

Schefuß, E., Sinninghe Damsté, J.S., Jansen, J.H.F., 2004. Forcing of tropical Atlantic sea surface temperatures during the mid-Pleistocene transition. Paleoceanography 19.

Schmieder, F., von Dobeneck, T., Bleil, U., 2000. The Mid-Pleistocene climate transition as documented in the deep South Atlantic Ocean: initiation, interim state and terminal event. Earth Planet. Sci. Lett. 179, 539–549.

Schulz, M., Mudelsee, M., 2002. REDFIT: estimating red-noise spectra directly from unevenly spaced paleoclimatic time series. Comput. Geosci. 28, 421–426.

Shackleton, N.J., 1974. Attainment of isotopic equilibrium between ocean water and the benthonic foraminifera genus Uvigerina: isotopic changes in the ocean during the last glacial. Colloques Internationaux du C.N.R.S. 219, 203–209.

Shackleton, N.J., Opdyke, N.D., 1973. Oxygen isotope and palaeomagnetic stratigraphy of equatorial Pacific core V28-238: oxygen isotope temperatures and ice volumes on a $10^5$ year and $10^6$ year scale. J. Quatern. Res. 3, 39–55.

Shackleton, N.J., Opdyke, N.D., 1976. In: Cline, R.M., Hays, J.D. (Eds.), Oxygen isotope and palaeomagnetic stratigraphy of Equatorial Pacific Core V28-239, Late Pliocene to Latest Pleistocene. : Investigations of Late Quaternary Paleoceanography and Paleoclimatology, 145. Geological Society of America Memoir, pp. 449–464.

Shackleton, N.J., Hall, M.A., Vincent, E., 2000. Phase relationships between millennial-scale events 64,000–24,000 years ago. Paleoceanography 15, 565–569.

Short, D.A., Mengel, J.D., Crowley, T.J., Hyde, W.T., North, G.R., 1991. Filtering of Milankovitch cycles by Earth's geography. Quatern. Res. 35, 157–173.

Skinner, L.C., Shackleton, N.J., Elderfield, H., 2003. Millennial-scale variability of deep-water temperature and δ18Odw indicating deep water source variations in the Northeast Atlantic, 0–34 cal. ka BP. Geochem. Geophys. Geosyst. 4, 1098 doi:1010.1029/2003GC000585. Q11

Sun, Y., Clemens, S.C., An, Z., Yu, Z., 2006. Astronomical timescale and palaeoclimatic implication of stacked 3.6-Myr monsoon records from the Chinese Loess Plateau. Quatern. Sci. Rev. 25, 33–48.

Wara, M.W., Ravelo, A.C., Revenaugh, J.S., 2000. The pacemaker always rings twice. Paleoceanography 15, 616–624.

Weirauch, D., Billups, K., Martin, P., 2008. Evolution of millennial-scale climate variability during the mid-Pleistocene. Paleoceanography 23, PA3216 doi:3210.1029/2007PA001584. Q12

Yashayaev, I., van Aken, H.M., Holliday, N.P., Bersch, M., 2007. Transformation of the Labrador Sea Water in the subpolar Norh Atlantic. Geophys. Res. Lett. 34, L22605 doi:22610.21029/22007GL031812. Q13


UNCORRECTED PROOF